24th INTERNATIONAL CONGRESS ON SOUND AND VIBRATION
23–27 July 2017, London

HARMONIC BALANCE COMPUTATION OF THE NONLINEAR FREQUENCY RESPONSE OF A THIN PLATE

Jongsuh Lee, Thibaut Detroux and Gaëtan Kerschen

University of Liège, Department of Aerospace and Mechanical Engineering, Liège, Belgium
email: G.Kerschen@ulg.ac.be

The harmonic balance method (HBM) is used to investigate the dynamical behavior of the geometrical nonlinear plate. The middle plane displacements are included in the plate in which the equations of motion are developed by the principle virtual work. Moreover, the nonlinear frequency response curves, or NFRCs, are obtained by a continuation method.
Keywords: Nonlinear plate, Harmonic balance method, Nonlinear frequency response curve

1. Introduction

When thin plates are subjected to large external loads, the plates experience a large amplitude of deflections; in other words, the plates exhibit geometrical nonlinear vibrations. Geometrical nonlinearity often occurs in aircraft skin-panels when the aircraft is subjected to high levels of aerodynamic forces. This nonlinearity, developed by in-plane membrane stresses in the plates, generally results in an increase of resonance frequencies (i.e., hardening effect) and changes of mode shapes with respect to external force levels. Extensive reviews on the nonlinear vibration of thin plates are given in Refs. [1-3], in which they introduced accurate formulas for the highly nonlinear large deformations.

Many researchers have analyzed the nonlinearity of plates using the continuum method [4] and the finite element method [5]. If the finite element model is subjected to harmonic excitation, the steady state periodic response can be estimated by the harmonic balance method (HBM) [6]. The HBM, or the Fourier-Galerkin method, is performed in the frequency domain. Recently, this method has been applied to nonlinear large scale structures such as a full scale vehicle, aircraft and bladed disk because HBM has much less computational burden than time domain methods [7-10].

The present study introduces finite element formulas for a thin plate that employed von Kármán's nonlinear strain-displacement relationships. In addition, the nonlinear frequency response curves (NFRCs) are obtained to confirm the changes in resonance frequencies with respect to the increase of external force levels. To this end, the HBM is applied to the finite element model. The analytic form of the Jacobian matrix, which is used in the HBM, is derived from the presented finite element formulas. The analytic form allows for improvement of computational efficiency, especially for large scale structures, compared to the finite difference method (FDM).

2. Theory

2.1 Equations of motion

The nonlinear strain-displacement relationships of von-Kármán are defined as follows:

$$\boldsymbol{\varepsilon}_L^p = \begin{Bmatrix} \dfrac{\partial u}{\partial x} \\ \dfrac{\partial v}{\partial y} \\ \dfrac{\partial u}{\partial y} + \dfrac{\partial v}{\partial x} \end{Bmatrix}, \ \boldsymbol{\varepsilon}_L^b = \begin{Bmatrix} -\dfrac{\partial^2 w}{\partial x^2} \\ -\dfrac{\partial^2 w}{\partial y^2} \\ -2\dfrac{\partial^2 w}{\partial x \partial y} \end{Bmatrix}, \ \boldsymbol{\varepsilon}_N^p = \begin{Bmatrix} \dfrac{1}{2}\left(\dfrac{\partial w}{\partial x}\right)^2 \\ \dfrac{1}{2}\left(\dfrac{\partial w}{\partial y}\right)^2 \\ \dfrac{\partial w}{\partial x}\dfrac{\partial w}{\partial y} \end{Bmatrix} \tag{1}$$

where $\boldsymbol{\varepsilon}_L^p$ and $\boldsymbol{\varepsilon}_L^b$ are the linear membrane and bending strains, and $\boldsymbol{\varepsilon}_N^p$ is the geometrically nonlinear membrane strain. u and v are in-plane displacements in x and y coordinates, and w is lateral displacement in z coordinate. The equations of motion can be derived from the virtual work principles:

$$\delta U + \delta T = \delta W \tag{2}$$

where

$$\delta U = \int_A \left[\delta\boldsymbol{\varepsilon}_L^{pT} \mathbf{D} \boldsymbol{\varepsilon}_L^p + \delta\boldsymbol{\varepsilon}_L^{pT} \mathbf{D} \boldsymbol{\varepsilon}_N^p + \delta\boldsymbol{\varepsilon}_N^{pT} \mathbf{D} \boldsymbol{\varepsilon}_L^p + \delta\boldsymbol{\varepsilon}_N^{pT} \mathbf{D} \boldsymbol{\varepsilon}_N^p \right] dA + \int_A \delta\boldsymbol{\varepsilon}_L^{bT} \mathbf{D}' \boldsymbol{\varepsilon}_L^b \, dA \tag{3}$$

$$\delta T = \int_A \rho h \left[\delta u \ddot{u} + \delta v \ddot{v} + \delta w \ddot{w} \right] dA \tag{4}$$

and

$$\delta T = \lfloor \delta u \ \delta v \ \delta w \rfloor \int_A [\mathbf{N}]^T \begin{Bmatrix} 0 \\ 0 \\ \mathbf{f}_w(x, y, t) \end{Bmatrix} dA \tag{5}$$

In Eq. (2), U, T and W are virtual works by the restoring forces, inertia and the external forces, respectively. **D** and **D′** are the membrane and flexural rigidity matrices, respectively. A is the area, and ρ and h are the mass density and the thickness, respectively. **N** is the shape function matrix and $\boldsymbol{f}_w$ is the external force vector in the transverse direction. In this study, only the external force in the transverse direction is considered. The superscript T denotes the transpose matrix. Substituting Eq. (1) into Eq. (2) and neglecting in-plane inertia yields the equations of motion:

$$\mathbf{M}_w \ddot{\mathbf{r}}_w + \mathbf{C}_w \dot{\mathbf{r}}_w + \mathbf{K}_L \mathbf{r}_w + \mathbf{K}_{NL}(\mathbf{w}) \mathbf{r}_w = \mathbf{f}_w \tag{6}$$

where

$$\mathbf{K}_{NL}(\mathbf{w}) = \mathbf{K}_4(\mathbf{w}) - \mathbf{K}_3(\mathbf{w}) \mathbf{K}_1^{p^{-1}} \mathbf{K}_2(\mathbf{w}) \tag{7}$$

In Eq. (6), **M** and **r** are the mass matrix and response vector, respectively, and viscous matrix **C** is introduced. Subscript w represents the transverse direction. $\mathbf{K}_L$ and $\mathbf{K}_{NL}$ are the linear and nonlinear bending stiffness matrices, respectively. Here, the nonlinear stiffness matrix is a quadratic function of the transverse displacement vector, $\boldsymbol{w}$. The detailed form of the nonlinear stiffness matrix is represented in Eq. (7). Here, $\mathbf{K}_2$ and $\mathbf{K}_3$ are the nonlinear stiffness matrices which linearly depend on $\mathbf{r}_w$ and $\mathbf{K}_4$ is the nonlinear matrix which quadratically depends on $\mathbf{r}_w$. It is noted that the equations of motion of a thin plate can be represented only by the transverse direction because the term "in-plane inertia" is neglected.

2.2 Harmonic Balance Method (HBM)

The present study presents only a summary of the HBM for the Jacobian matrix. More detailed information regarding the HBM can be found in the reference [10]. The equations of motion (6) can be transformed to the following:

$$\mathbf{M}_w\ddot{\mathbf{r}}_w + \mathbf{C}_w\dot{\mathbf{r}}_w + \mathbf{K}_L\mathbf{r}_w = \mathbf{f}_w(\omega,t) - \mathbf{f}_{NL}(\mathbf{r}_w) = \mathbf{f}(\omega,t,\mathbf{r}_w) \tag{8}$$

where $\mathbf{f}_{\mathrm{NL}}$ represents the nonlinear force vector by the nonlinear stiffness matrix and the transverse displacement vector. $\mathbf{f}$ is the general force vector, including the linear and nonlinear forces. The assumed periodic solutions, $\mathbf{r}_{\mathrm{W}}$ and $\mathbf{f}$, are approximated by Fourier series truncated to the N$^{\mathrm{th}}$ harmonic:

$$\begin{aligned}\mathbf{r}_w(t) &= \mathbf{c}_0^r + \sum_{k=1}^{N_H}\left(\mathbf{s}_k^r \sin(k\omega t) + \mathbf{c}_k^r \cos(k\omega t)\right)\\ \mathbf{f}(t) &= \mathbf{c}_0^f + \sum_{k=1}^{N_H}\left(\mathbf{s}_k^f \sin(k\omega t) + \mathbf{c}_k^f \cos(k\omega t)\right)\end{aligned} \tag{9}$$

where $\mathbf{s}_{\mathrm{k}}$ and $\mathbf{c}_{\mathrm{k}}$ are vectors of the Fourier coefficients to the sine and cosine terms, respectively. Further, the superscripts r and f stand for the response and force terms, respectively. ω is the external excitation frequency. Substituting Eq. (9) into Eq. (8) and following simple manipulations yields the following:

$$\mathbf{h}(\mathbf{z},\omega) \equiv \mathbf{A}(\omega)\mathbf{z} - \mathbf{b}(\mathbf{z},\omega) = \mathbf{0} \tag{10}$$

$\mathbf{A}$ is the matrix describing the linear dynamics of the plate and its size: $(2N_H+1)n \times (2N_H+1)n$. $\mathbf{z}$ is the coefficient vector which consists of the Fourier coefficients of the displacement $\mathbf{r}_{\mathrm{W}}$ and force $\mathbf{f}$. Detailed forms of the matrix and vectors in Eq. (10) can be found in Ref. [10]. Eq. (10) is nonlinear because $\mathbf{b}$ is a function of $\mathbf{z}$. Therefore, it must be solved using an iterative method (e.g., Newton-Raphson) in which the Jacobian matrix must be calculated at each iteration. The Jacobian matrix of Eq. (10) with respect to the Fourier coefficient vector $\mathbf{z}$ can be represented as follows:

$$\mathbf{J}_z = \frac{\partial\mathbf{h}}{\partial\mathbf{z}} = \mathbf{A} - \frac{\partial\mathbf{b}}{\partial\mathbf{z}} \tag{11}$$

The resultant matrix by the derivative between the displacement and force coefficient vectors can be expressed by the chain rule:

$$\frac{\partial\mathbf{b}}{\partial\mathbf{z}} = \frac{\partial\mathbf{b}}{\partial\bar{\mathbf{f}}}\frac{\partial\bar{\mathbf{f}}}{\partial\bar{\mathbf{r}}}\frac{\partial\bar{\mathbf{r}}}{\partial\mathbf{z}} = \boldsymbol{\Gamma}^{+}\frac{\partial\bar{\mathbf{f}}}{\partial\bar{\mathbf{r}}}\boldsymbol{\Gamma} \text{ where } \bar{\mathbf{r}} = \begin{Bmatrix} r_{w1}(t_1)\\ \vdots \\ r_{w1}(t_N)\\ \vdots \\ r_{wn}(t_1)\\ \vdots \\ r_{wn}(t_N)\end{Bmatrix},\ \bar{\mathbf{f}} = \begin{Bmatrix} f_1(t_1)\\ \vdots \\ f_1(t_N)\\ \vdots \\ f_n(t_1)\\ \vdots \\ f_n(t_N)\end{Bmatrix} \tag{12}$$

Where $\bar{\mathbf{r}}$ and $\bar{\mathbf{f}}$ are the newly defined vectors, including N number of concatenated responses and forces for all DOFs. $\boldsymbol{\Gamma}^{+}$ and $\boldsymbol{\Gamma}$ show the relationship between the coefficient vectors in the time and frequency domains; thus, $\boldsymbol{\Gamma}^{+}$ and $\boldsymbol{\Gamma}$ can be interpreted as operators for the Fourier and inverse Fourier transforms, respectively. Here, the superscript + represents the Moore-Penrose pseudo-inverse. The two operators can be expressed using explicit formulas [10]. Assuming the external forces are independent of the responses, the terms in the thin plate corresponding to the resultant matrix by the derivative between the vectors of $\bar{\mathbf{r}}$ and $\bar{\mathbf{f}}$ in Eq. (12) can be represented only by the nonlinear force term. The derivative of the nonlinear force vector with respect to the transverse displacement in the thin plate is as follows:

$$\frac{\partial\mathbf{f}_{\mathrm{NL}}}{\partial\mathbf{r}_w} = \left(\frac{\partial\mathbf{K}_{NL}(\mathbf{r}_w)}{\partial\mathbf{r}_w}\mathbf{r}_w + \mathbf{K}_{NL}(\mathbf{r}_w)\right) \tag{13}$$

where

$$\frac{\partial \mathbf{K}_{NL}(\mathbf{r}_w)}{\partial \mathbf{r}_w} = \left(\frac{\partial \mathbf{K}_4(\mathbf{r}_w)}{\partial \mathbf{r}_w} - \frac{\partial \mathbf{K}_3(\mathbf{r}_w)}{\partial \mathbf{r}_w} \mathbf{K}_1^{p^{-1}} \mathbf{K}_2(\mathbf{r}_w) - \mathbf{K}_3(\mathbf{r}_w) \mathbf{K}_1^{p^{-1}} \frac{\partial \mathbf{K}_2(\mathbf{r}_w)}{\partial \mathbf{r}_w} \right) \tag{14}$$

Consequently, Eq. (13) is the analytic expression of the Jacobian matrix for a thin plate. And, as shown in Eq. (14), the third order tensor must be managed in order to compute the Jacobian matrix. The nonlinear response corresponding to the excitation frequency is computed by the continuation procedure.

3. Case study

The proposed method is demonstrated on a thin, rectangular plate in which the clamped-clamped boundary conditions are imposed on the left and right sides, as shown in Fig. 1. The defined properties and parameters are as follows:

Geometric properties: a = 600 mm, b = 50 mm and h = 1 mm.

Material properties: E = 2e10 N/m^2, ρ = 7980 kg/m^3 and ν = 0.33.

External force levels: F_w = 5e-4 N, 8e-4 N and 1e-3 N.

External forcing location: x = 120 mm, y = 25 mm.

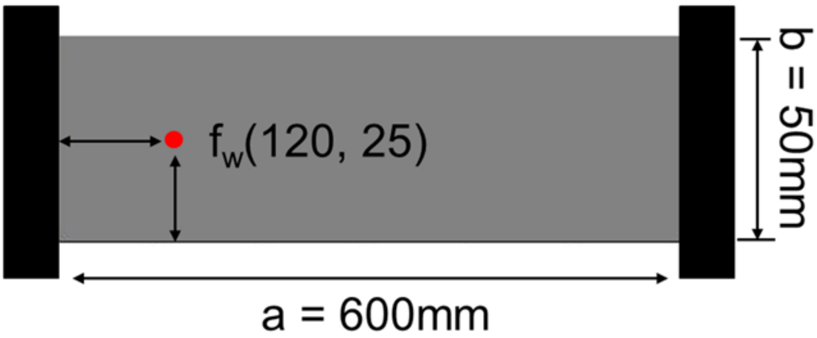

Fig. 1. Configuration of thin plate

Prior to performing simulations, a process was conducted to verify the derived analytic form of the Jacobian matrix. The Jacobian matrices were evaluated using the derived analytic formula and by the FDM when the smallest force among the defined levels is applied. Moreover, ten arbitrary elements were selected in both cases of the analytic formula and of the FDM on the same locations of the Jacobian matrices.

Table 1. The Jacobian matrices estimated by the analytic formula versus by the FDM

Analytic Formula	FDM	Error (%)
-8434688.818	-8435650.46	0.011
-5919363.77	-5918966.21	0.006
-19266242.8	-19264043.5	0.011
-5919362.8	-5921317.8	0.033
-8434687.81	-8435257.69	0.006
-8455452.28	-8455446.39	6.97E-05
-5768988.81	-5771214.04	0.038
-19257163.7	-19256256	0.004
-5768987.88	-5768803.58	0.003
-8455451.277	-8455605.02	0.001

As shown in Table 1, the differences in the estimated values between the two methods are less than 1% across the elements. Thus, the validity of the proposed method was confirmed. The NFRCs corresponding to the external force levels were obtained at the forcing location (i.e., point FRFs).

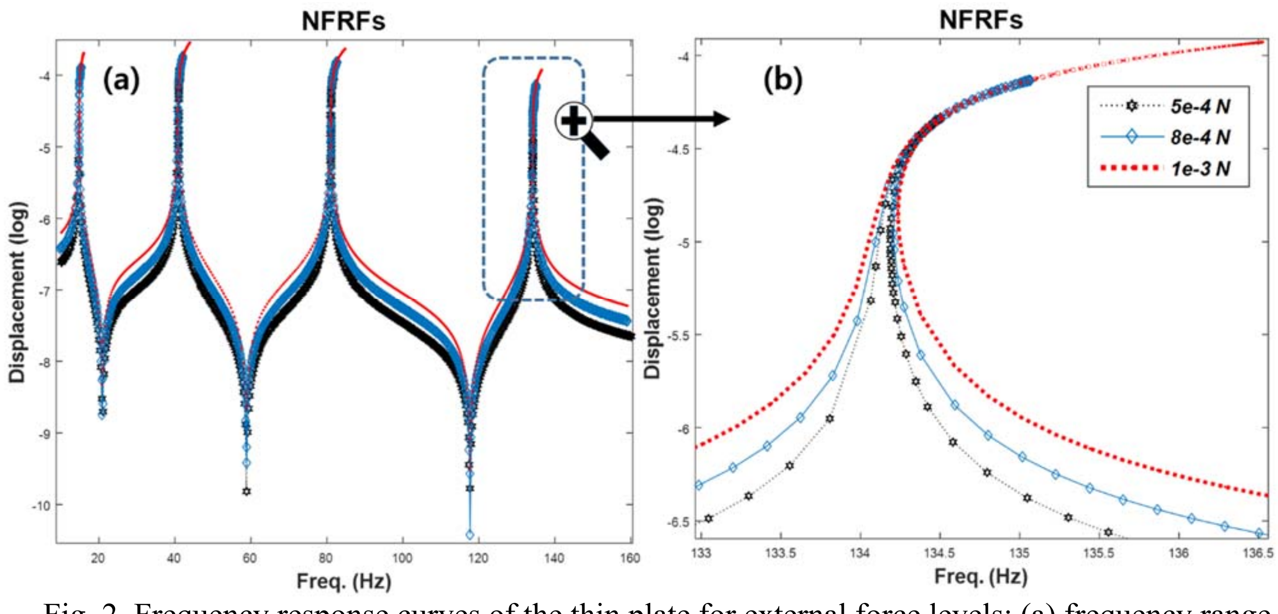

Fig. 2. Frequency response curves of the thin plate for external force levels: (a) frequency range from 10 to 160 (b) zoomed frequency range near 4th mode

Fig. 2 shows the obtained frequency response curves for the defined external force levels, and their magnitudes are shown in log scale. As shown in the figure, the resonance frequency of each mode increases as the external force level increases. The results, displayed in the figure, confirmed the expected hardening effect.

4. Conclusion

The present study introduced the numerical model of a thin plate, in which the geometrical non-linearity is included, and reviewed the use of HBM for analyzing dynamic characteristics of the plate. In addition, the relationship between the forces and the responses was presented in the analytic form to obtain the Jacobian matrix that is used in the HBM. Simulations were conducted to verify the introduced analytic form, and the proposed method was verified by comparing its results with those obtained from the FDM. Lastly, the hardening effect was confirmed through the obtained NFRCs at the defined external forces.

5. Acknowledgement

This work was fully supported by the European Commission of Marie Curie COFUND (600405).

REFERENCES

1 M. Sathyamoorthy, "Nonlinear vibration analysis of plates: a review and survey of current developments," *Applied Mechanics Reviews,* vol. 40, pp. 1553-1561, 1987.

2 C.-Y. Chia, "Geometrically nonlinear behavior of composite plates: a review," *Applied Mechanics Reviews,* vol. 41, pp. 439-451, 1988.

3 W. Lacarbonara and M. Pasquali, "A geometrically exact formulation for thin multi-layered laminated composite plates: theory and experiment," *Composite Structures,* vol. 93, pp. 1649-1663, 2011.

4 N. Yamaki, "Influence of large amplitudes on flexural vibrations of elastic plates," *Journal of Applied Mathematics and Mechanics,* pp. 501-510, 1961.

5 C. Mei, "Nonlinear vibration of beams by matrix," *Computers & Structures,* vol. 3, no. 1, pp. 163-174, 1973.

6 P. Ribeiro and M. Petyt, "Multi modal geometrical nonlinear free vibration of fully clamped composite laminated plates," *Journal of Sound and Vibration,* vol. 225, no. 1, pp. 127-152, 1999.

7 F. Barillon, J. Sinou, J. Duffal and L. Jézéquel, "Non-linear dynamics of a whole vehicle finite element model using a harmonic balance method," *International Journal of Vehicle Design,* vol. 63, no. 4, pp. 387-403, 2009.

8 A. Sénéchal, B. Petitjean and L. Zoghaib, "Development of a numerical tool for industrial structures with local nonlinearities," *International Conference on Noise and Vibration Engieering ISMA 2014*, Leuven.

9 M. Krack, L. P.-v. Scheidt, J. Wallaschek, C. Siewert and A. Hartung, "Reduced order modeling based on complex nonlinear modal analysis and its application to bladed disks with shroud contact," *Journal of Engineering for Gas Turbines and Power,* vol. 135, pp. 1-8, 2013.

10 T. Detroux, L. Renson, L. Masset and G. Kerschen, "The harmonic balance method for bifurcation analysis of large sclae nonlinear mechanical systems," *Computer methods in applied mechanics and engineering,* vol. 296, pp. 18-38, 2015.